Article published online: 2024-06-06

Predictors for the Differentiation between Glioblastoma, Primary Central Nervous System Lymphoma, and Metastasis in Patients with a Solitary Enhancing Intracranial Mass

Pornthida Chuthip[1,2] Bunpot Sitthinamsuwan[1] Theerapol Witthiwej[1] Chottiwat Tansirisithikul[1] Inthira Khumpalikit[1] Sarun Nunta-aree[1]

[1] Division of Neurosurgery, Department of Surgery, Faculty of Medicine Siriraj Hospital, Mahidol University, Bangkok, Thailand
[2] Department of Surgery, Pattani Hospital, Pattani, Thailand

Address for correspondence Bunpot Sitthinamsuwan, MD, Division of Neurosurgery, Department of Surgery, Faculty of Medicine, Siriraj Hospital, Mahidol University, 2 Wang Lang Road, Bangkok Noi, Bangkok 10700, Thailand (e-mail: bunpotsi@yahoo.com).

Asian J Neurosurg 2024;19:186–201.

Abstract

Introduction Differentiation between glioblastoma (GBM), primary central nervous system lymphoma (PCNSL), and metastasis is important in decision-making before surgery. However, these malignant brain tumors have overlapping features. This study aimed to identify predictors differentiating between GBM, PCNSL, and metastasis.

Materials and Methods Patients with a solitary intracranial enhancing tumor and a histopathological diagnosis of GBM, PCNSL, or metastasis were investigated. All patients with intracranial lymphoma had PCNSL without extracranial involvement. Demographic, clinical, and radiographic data were analyzed to determine their associations with the tumor types.

Results The predictors associated with GBM were functional impairment ($p = 0.001$), large tumor size ($p < 0.001$), irregular tumor margin ($p < 0.001$), heterogeneous contrast enhancement ($p < 0.001$), central necrosis ($p < 0.001$), intratumoral hemorrhage ($p = 0.018$), abnormal flow void ($p < 0.001$), and hypodensity component on noncontrast cranial computed tomography (CT) scan ($p < 0.001$). The predictors associated with PCNSL comprised functional impairment ($p = 0.005$), deep-seated tumor location ($p = 0.006$), homogeneous contrast enhancement ($p < 0.001$), absence of cystic appearance ($p = 0.008$), presence of hypointensity component on precontrast cranial T1-weighted magnetic resonance imaging (MRI; $p = 0.027$), and presence of isodensity component on noncontrast cranial CT ($p < 0.008$). Finally, the predictors for metastasis were an infratentorial ($p < 0.001$) or extra-axial tumor location ($p = 0.035$), smooth tumor margin ($p < 0.001$), and presence of isointensity component on cranial fluid-attenuated inversion recovery MRI ($p = 0.047$).

Conclusion These predictors may be used to differentiate between GBM, PCNSL, and metastasis, and they are useful in clinical management.

Keywords
- glioblastoma
- brain metastasis
- primary central nervous system lymphoma (PCNSL)
- predictor
- differentiation

article published online
June 6, 2024

DOI https://doi.org/10.1055/s-0044-1787051.
ISSN 2248-9614.

Thieme Medical and Scientific Publishers Pvt. Ltd., A-12, 2nd Floor, Sector 2, Noida-201301 UP, India

Introduction

A solitary contrast-enhancing brain lesion is a usual finding of neoplastic diseases of the brain, including malignant brain tumors.[1] The common malignant lesions of the brain are glioblastoma (GBM), primary central nervous system lymphoma (PCNSL), and metastasis.[2] Contrast-enhanced neuroimaging studies play a major role in the differentiation and diagnosis of these tumors. Nevertheless, overlapping neuroradiological features of these malignant neoplasms are occasionally seen, resulting in a difficult diagnosis.[2,3]

Preoperative differentiation between GBM, PCNSL, and metastasis is useful in clinical situations, because the treatments for these tumors are different. Complete resection is the primary therapy for GBM, whereas PCNSL requires a tissue biopsy, followed by high-dose chemotherapy with or without radiation therapy.[4–6] In patients with a single accessible metastatic brain tumor who have a favorable performance status and a well-controlled primary cancer, surgical removal is a good treatment option for improving the survival and neurological condition of these patients.

The aim of this study was to identify the predictors differentiating between GBM, PCNSL, and metastasis in patients presenting with a solitary contrast-enhancing intracranial tumor.

Materials and Methods

Patient Population

This cross-sectional study recruited individuals who had a histopathological diagnosis of GBM, PCNSL, or metastasis and had a solitary contrast-enhancing intracranial tumor. The tumors had been revealed by cranial computed tomography (CT) or magnetic resonance imaging (MRI) scanning. All patients underwent cranial CT and head MRI was performed in some cases. The enrolled patients were operated at the Division of Neurosurgery, Department of Surgery, Faculty of Medicine Siriraj Hospital, Bangkok, Thailand. In all cases, a craniotomy with resection or stereotactic biopsy of the tumor was performed. The tumors of individuals with intracranial lymphoma primarily occurred in an intracranial location with no extracranial involvement. Prior to the surgery for the intracranial tumors, none of the included patients had ever undergone brain surgery or received radiation therapy to the brain. Patients who underwent surgery for residual tumors were excluded from the research to avoid confounding features in radiographic studies of the brain. This work was approved by the Siriraj Institutional Review Board, Faculty of Medicine Siriraj Hospital, Mahidol University, Thailand. The study has been conducted in accordance with the principles set forth in the Helsinki Declaration.

Data Collection

The gathered data comprised demographic characteristics, clinical information, and radiographic features. The demographic characteristics were age, gender, and histopathological diagnosis. The clinical manifestations (increased intracranial pressure, seizure, focal neurological deficit, and functional impairment) and their duration prior to surgery were collected from outpatient and inpatient records. Focal neurological deficit is defined as an impairment of the focal neurological function, such as hemiparesis, dysphasia, or visual field deficit. Functional impairment is defined as limitations of patients' functions due to the disease (patients may not achieve certain functions in their daily life, and there may be limitations in social and occupational aspects). The radiographic features consisted of the tumor size, presence and degree of perilesional brain edema and midline shift, tumor location, characteristics of the tumor margin and contrast enhancement, presence of cystic appearance, central necrosis, intratumoral hemorrhage, aberrant flow void, leptomeningeal enhancement, hydrocephalus, and involvement of the skull. The tumor size was measured by a maximum diameter in any dimension of contrast-enhanced lesion on postcontrast neuroimaging. The degree of perilesional brain edema was calculated by a maximum diameter in any dimension of peritumoral hypodensity area on postcontrast cranial CT or peritumoral hyperintensity area on T2-weighted (T2W) cranial MRI. The tumor characteristics revealed by the cranial CT and MRI scanning and the relative cerebral blood volume (rCBV) were also analyzed. The radiographic variables were independently interpreted by two experienced neurosurgeons (P.C. and B.S.). The variables with discordance between the interpreters were totally collected for decision-making of agreement by both interpreters. Eventually, concordance of all variables was achieved. All values of the rCBV were evaluated by neuroradiologists and the data were obtained from MRI reports. However, some information was unavailable for some patients. Thus, the case numbers (n) of some variables were different from most.

Statistical Analysis

All data were analyzed using the IBM SPSS Statistics for Windows (version 24.0; IBM Corp., Armonk, New York, United States). Demographic data were analyzed using descriptive statistics. The analyses of the associations between the variables and the types of tumors were performed using either the Pearson's chi-squared test or the Fisher's exact test. The strengths of association were calculated using odds ratios (OR) and 95% confidence intervals (95% CI). The Kruskal–Wallis test was used to investigate differences in the ages, tumor sizes, degrees of peritumoral brain edema, and midline shift of the tumor groups. A p-value of less than 0.05 was deemed statistically significant. Furthermore, sensitivity, specificity, positive likelihood ratio (LR+), negative likelihood ratio (LR−), positive predictive value (PPV), negative predictive value (NPV), and accuracy of individual statistically significant variables were presented.

Results

In all, 138 patients were enrolled. Sixty-two cases (44.9%) were GBM, 23 (16.7%) were PCNSL, and 53 (38.4%) were metastasis. There were 70 males (50.7%) and 68 females (49.3%), with a median age of 57 years (range, 15–81 years).

The most common clinical manifestation was focal neurological deficit (114 patients; 82.6%), whereas increased intracranial pressure was the second most common symptom (60 patients; 43.5%). Seizure was a dominant clinical feature of the GBM group, whereas functional impairment was obvious in the GBM and PCNSL groups. There were no differences in the durations of the symptoms of the three groups.

The tumor size was significantly larger for the GBM group than the other groups ($p < 0.001$). In terms of the degree of perilesional brain edema and midline shift, there was no significant difference between the groups. As to the tumor location, the infratentorial location was the most common in cases of metastasis but exceedingly rare for the GBM group ($p < 0.001$). With the PCNSL group, the supratentorial location was the most common. Tumors with an extra-axial location were rare in all groups and were exclusively found in the metastatic group ($p = 0.035$). A tumor arising in a deep-seated location was the hallmark of the PCNSL group ($p = 0.006$), whereas tumors with a smooth margin were obviously found in the metastatic group ($p < 0.001$). After contrast injection, the tumors of most PCNSL patients showed a homogeneous contrast enhancement, whereas the tumors in almost all the GBM patients and the majority of the metastatic group demonstrated a heterogeneous contrast enhancement ($p < 0.001$). The PCNSL group had no cystic appearance ($p = 0.008$) and had exceedingly rare intratumoral hemorrhage ($p = 0.018$). In the GBM group, the significant characteristics were the presence of central necrosis ($p < 0.001$) and abnormal flow void ($p < 0.001$). As to the precontrast cranial MRI studies, most tumors in the GBM group showed the presence of hypointensity component ($p = 0.027$) on T1-weighted (T1W) MRI. Furthermore, we found that the presence of isointensity component of tumors on fluid-attenuated inversion recovery (FLAIR) sequence was apparently found in metastasis ($p = 0.047$). There was a significant difference in the number of cases with the presence of hypodensity component of tumor in the noncontrast-enhanced cranial CT scans ($p < 0.001$). In the PCNSL group, there was a predominance of tumors with isodensity component in the noncontrast-enhanced cranial CT scans ($p = 0.008$). There were no significant differences in the incidences of perilesional brain edema, midline shift, leptomeningeal enhancement, hydrocephalus, skull involvement, characteristic of tumor flow void, and degree of rCBV of the three tumor groups. The associations between the demographic, clinical, and radiographic variables and the types of tumors are detailed in ►**Table 1**.

In an analysis of the strengths of association (►**Table 2**), the factors with a significant association with GBM were functional impairment (OR, 5.0; 95% CI, 1.6–15.9; $p = 0.004$), central necrosis (OR, 8.0; 95% CI, 3.4–18.5; $p < 0.001$), intratumoral hemorrhage (OR, 11.3; 95% CI, 1.4–89.5; $p = 0.010$), abnormal flow void (OR, 14.5; 95% CI, 3.1–67.5; $p < 0.001$), presence of

Table 1 The associations between the demographic, clinical, and radiographic variables and the tumor types

Variables	Analyzed cases (*n*)	Histopathology			*p*-Value
		GBM	PCNSL	Metastasis	
Total numbers (%)	138	62 (44.9%)	23 (16.7%)	53 (38.4%)	
Age (y), median (range)	138	58 (15–79)	64 (35–78)	56 (30–81)	0.083
Gender, *n* (%)	138				0.096
Male		35 (56.5%)	7 (30.4%)	28 (52.8%)	
Female		27 (43.5%)	16 (69.6%)	25 (47.2%)	
Clinical manifestation, *n* (%)	138				
Increased intracranial pressure		24 (38.7%)	8 (34.8%)	28 (52.8%)	0.205
Seizure		15 (24.2%)	1 (4.3%)	5 (9.4%)	0.025[a]
Focal neurological deficit[b]		52 (83.9%)	22 (95.7%)	40 (75.5%)	0.097
Functional impairment[c]		18 (29.0%)	8 (34.8%)	4 (7.5%)	0.005[a]
Duration of symptoms (d), median (range)	138	21 (1–240)	14 (6–120)	21 (1–90)	0.418
Tumor size (mm), median (range)	138	51 (14–76)	42 (10–61)	36 (15–90)	<0.001[a]
Tumor location A[d], *n* (%)	138				<0.001[a]
Supratentorial		61 (98.4%)	21 (91.3%)	36 (67.9%)	
Infratentorial		1 (1.6%)	2 (8.7%)	17 (32.1%)	
Tumor location B[e], *n* (%)	138				0.035[a]
Intra-axial		62 (100.0%)	23 (100.0%)	49 (92.5%)	
Extra-axial		0 (0.0%)	0 (0.0%)	4 (7.5%)	
Tumor location C[f], *n* (%)	138				0.006[a]
Superficial		53 (85.5%)	16 (69.6%)	51 (96.2%)	
Deep-seated		9 (14.5%)	7 (30.4%)	2 (3.8%)	
Tumor margin, *n* (%)	138				<0.001[a]
Smooth		13 (21%)	10 (43.5%)	30 (56.6%)	

Table 1 (*Continued*)

Variables	Analyzed cases (*n*)	Histopathology			*p*-Value
		GBM	PCNSL	Metastasis	
Irregular		49 (79%)	13 (56.5%)	23 (43.4%)	
Contrast enhancement, *n* (%)	138				<0.001[a]
Homogeneous		1 (1.6%)	14 (60.9%)	7 (13.2%)	
Heterogeneous		61 (98.4%)	9 (39.1%)	46 (86.8%)	
Cystic appearance, *n* (%)	138	19 (30.6%)	0 (0%)	17 (32.1%)	0.008[a]
Central necrosis, *n* (%)	138	49 (79%)	9 (39.1%)	17 (32.1%)	<0.001[a]
Intratumoral hemorrhage, *n* (%)	138	21 (33.9%)	1 (4.3%)	12 (22.6%)	0.018[a]
Perilesional brain edema, *n* (%)	138	54 (87.1%)	22 (95.7%)	46 (86.6%)	0.493
Degree of brain edema (mm), median (range)	138	36 (15–60)	38 (17–61)	32 (13–61)	0.214
Midline shift, *n* (%)	138	43 (69.4%)	12 (52.2%)	28 (52.8%)	0.136
Degree of midline shift (mm), median (range)	138	8 (2–18)	9 (3–15)	7 (3–19)	0.763
Abnormal flow void, *n* (%)	138	36 (58.1%)	2 (8.7%)	10 (18.9%)	<0.001[a]
Characteristic of flow void, *n* (%)	48				0.295
Intratumoral		8 (22.2%)	1 (50%)	5 (50%)	
Peritumoral		22 (61.1%)	1 (50%)	5 (50%)	
Both		6 (16.7%)	0 (0%)	0 (0%)	
Leptomeningeal enhancement, *n* (%)	138	9 (14.5%)	1 (4.3%)	6 (11.3%)	0.428
Hydrocephalus, *n* (%)	138	14 (22.6%)	2 (8.7%)	15 (28.3%)	0.170
Skull involvement, *n* (%)	138	0 (0%)	0 (0%)	3 (5.7%)	0.127
Tumor characteristic on precontrast T1W MRI, *n* (%)	57				
Presence of hypointensity component		29 (90.6%)	8 (72.7%)	8 (57.1%)	0.027[a]
Presence of isointensity component		19 (59.4%)	7 (63.6%)	11 (78.6%)	0.555
Presence of hyperintensity component		0 (0.0%)	0 (0.0%)	2 (14.3%)	0.091
Tumor characteristic on T2W MRI, *n* (%)	57				
Presence of hypointensity component		4 (12.5%)	0 (0.0%)	4 (28.6%)	0.140
Presence of isointensity component		9 (28.1%)	2 (18.2%)	7 (50.0%)	0.253
Presence of hyperintensity component		32 (100.0%)	10 (90.9%)	12 (85.7%)	0.079
Tumor characteristic on FLAIR MRI, *n* (%)	57				
Presence of hypointensity component		1 (3.1%)	0 (0.0%)	3 (21.4%)	0.075
Presence of isointensity component		4 (12.5%)	1 (9.1%)	6 (42.9%)	0.047[a]
Presence of hyperintensity component		31 (96.9%)	10 (90.9%)	12 (85.7%)	0.287
Tumor characteristic on NCECT, *n* (%)	81				
Presence of hypodensity component		29 (96.7%)	6 (50.0%)	32 (82.1%)	<0.001[a]
Presence of isodensity component		12 (40.0%)	11 (91.7%)	24 (61.5%)	0.008[a]
Presence of hyperdensity component		8 (26.7%)	1 (8.3%)	8 (20.5%)	0.466
rCBV, *n* (%)	42				0.391
High		23 (95.8%)	8 (88.9%)	8 (88.9%)	
Normal		0 (0%)	1 (11.1%)	1 (11.1%)	
Low		1 (4.2%)	0 (0%)	0 (0%)	

Abbreviations: FLAIR, fluid-attenuated inversion recovery; GBM, glioblastoma; MRI, magnetic resonance imaging; *n*, number of cases; NCECT, noncontrast-enhanced computerized tomography; PCNSL, primary central nervous system lymphoma; rCBV, relative cerebral blood volume; T1W, T1-weighted; T2W, T2-weighted.

[a]Statistical significance.

[b]Focal neurological deficit is defined as an impairment of the focal neurological function, such as hemiparesis, dysphasia, or visual field deficit.

[c]Functional impairment is defined as limitations of patients' functions due to the disease (patients may not achieve certain functions in their daily life, and there may be limitations in social and occupational aspects).

[d]Tumor location A is categorized into supratentorial and infratentorial locations.

[e]Tumor location B is categorized into intra-axial and extra-axial locations.

[f]Tumor location C is categorized into superficial locations (cortical or subcortical region, epidural, or subdural space) and deep-seated locations (periventricular region, basal ganglia, thalamus, corpus callosum, or brainstem).

Table 2 The strengths of association between the variables and tumor types

Variables/ tumor types	Odds ratio (95% CI)	*p*-Value
Seizure		
PCNSL	1.0	
Metastasis	2.3 (0.25–20.8)	0.661
GBM	7.0 (0.9–56.6)	0.058
Functional impairment[b]		
Metastasis	1.0	
GBM	5.0 (1.6–15.9)	0.004[a]
PCNSL	6.5 (1.7–24.8)	0.005[a]
Infratentorial tumor location		
GBM	1.0	
PCNSL	5.8 (0.5–67.4)	0.177
Metastasis	28.8 (3.7–225.7)	<0.001[a]
Deep-seated tumor location[c]		
Metastasis	1.0	
GBM	4.3 (0.9–21.0)	0.062
PCNSL	11.2 (2.1–59.2)	0.003[a]
Smooth tumor margin		
GBM	1.0	
PCNSL	2.9 (1.0–8.1)	0.054
Metastasis	4.9 (2.2–11.1)	<0.001[a]
Homogeneous contrast enhancement		
GBM	1.0	
Metastasis	9.3 (1.1–78.1)	0.023[a]
PCNSL	94.9 (11.1–811.5)	<0.001[a]
Central necrosis		
Metastasis	1.0	
PCNSL	1.4 (0.5–3.8)	0.604
GBM	8.0 (3.4–18.5)	<0.001[a]
Intratumoral hemorrhage		
PCNSL	1.0	
Metastasis	6.4 (0.8–52.8)	0.094
GBM	11.3 (1.4–89.5)	0.010[a]
Abnormal flow void		
PCNSL	1.0	
Metastasis	2.4 (0.5–12.2)	0.327
GBM	14.5 (3.1–67.5)	<0.001[a]
Presence of hypointensity component on precontrast T1W MRI		
Metastasis	1.0	
PCNSL	2.0 (0.4–10.9)	0.677
GBM	7.3 (1.5–35.6)	0.015[a]
Presence of isointensity component on FLAIR MRI		
GBM	1.0	
PCNSL	1.4 (0.1–14.4)	0.762
Metastasis	5.3 (1.2–23.3)	0.029[a]
Presence of hypodensity component on NCECT		
PCNSL	1.0	
Metastasis	4.6 (1.1–18.5)	0.053
GBM	29.0 (2.9–287.0)	0.001[a]
Presence of isodensity component on NCECT		
GBM	1.0	
Metastasis	2.4 (0.9–6.4)	0.093
PCNSL	16.5 (1.9–145.0)	0.005[a]

Abbreviations: CI, confidence interval; FLAIR, fluid-attenuated inversion recovery; GBM, glioblastoma; MRI, magnetic resonance imaging; NCECT, noncontrast-enhanced computerized tomography; PCNSL, primary central nervous system lymphoma; T1W, T1-weighted.

[a]Statistical significance.

[b]Functional impairment is defined as limitations of patients' functions due to the disease (patients may not achieve certain functions in their daily life, and there may be limitations in social and occupational aspects).

[c]Deep-seated location refers to an area located at the deep part of the brain (the periventricular region, basal ganglia, thalamus, corpus callosum, or brainstem).

hypointensity component on cranial T1W MRI (OR, 7.3; 95% CI, 1.5–35.6; $p = 0.015$), and hypodensity component on cranial noncontrast-enhanced CT (OR, 29.0; 95% CI, 2.9–287.0; $p = 0.001$). In the case of PCNSL, the predicting factors for this type of tumor were functional impairment (OR, 6.5; 95% CI, 1.7–24.8; $p = 0.005$), deep-seated tumor location (OR, 11.2; 95% CI, 2.1–59.2; $p = 0.003$), homogeneous contrast enhancement (OR, 94.9; 95% CI, 11.1–811.5; $p < 0.001$), and presence of isodensity component of cranial noncontrast-enhanced CT (OR, 16.5; 95% CI, 1.9–145.0; $p = 0.005$). The factors indicating a high association with metastasis were infratentorial tumor location (OR, 28.8; 95% CI; 3.7–225.7; $p < 0.001$), smooth tumor margin (OR, 4.9; 95% CI; 2.2–11.1; $p < 0.001$), and homogeneous contrast enhancement (OR, 9.3; 95% CI, 1.1–78.1; $p = 0.023$).

Additionally, the individual categorical variable with statistical significance in ►**Table 1** was analyzed in terms of sensitivity, specificity, LR+, LR−, PPV, NPV, and accuracy. Results of the analysis are demonstrated in ►**Table 3**. Numerous variables showed dominant positive (supporting) and negative (opposing) possibilities of being GBM, PCNSL, or metastasis. For instance, in the variable of homogeneous contrast enhancement on neuroimaging studies, PCNSL revealed high specificity, LR+, NPV, and accuracy, whereas GBM showing low sensitivity, LR+, PPV, and accuracy. These results supported that tumor showing homogenous contrast enhancement on neuroimaging studies were likely to be

Table 3 Sensitivity, specificity, positive likelihood ratio, negative likelihood ratio, positive predictive value, negative predictive value, and accuracy of individual variable in differentiation of the tumor types

Variables	Sensitivity (%)	Specificity (%)	LR+	LR−	PPV (%)	NPV (%)	Accuracy (%)
Seizure							
GBM	24.2	92.1[a]	3.1	0.8	71.4[a]	59.9	61.6
PCNSL	4.4[b]	82.6	0.3	1.2	4.8[b]	81.2[b]	69.5
Metastasis	9.4	81.2	0.5	1.1	23.8	59.0	53.6
Functional impairment							
GBM	29.0	84.2	1.8	0.8	60.0	59.3	59.4
PCNSL	34.8	80.9	1.8	0.8	26.7	86.1[a]	73.2[a]
Metastasis	7.6	69.4	0.3	1.3	13.3	54.6	45.7
Infratentorial tumor location							
GBM	1.6[b]	75.0	0.1[b]	1.3	5.0[b]	48.3	42.1
PCNSL	8.7	84.4	0.6	1.1	10.0	82.2	71.7
Metastasis	32.1	96.5[a]	9.1[a]	0.7	85.0[a]	69.5	71.7
Deep-seated tumor location							
GBM	14.5	88.2	1.2	1.0	50.0	55.9	55.1
PCNSL	30.4	90.4[a]	3.2	0.8	39.0	86.6[a]	80.4[a]
Metastasis	3.8[b]	81.2	0.2[b]	1.2	11.1[b]	57.5	51.5
Smooth tumor margin							
GBM	20.3	47.4	0.4	1.7	24.5	42.4	35.5
PCNSL	43.5	62.6	1.2	0.9	18.9	84.7[a]	59.4
Metastasis	56.6	72.9[a]	2.1	0.6	56.6	73.0	66.7
Homogeneous contrast enhancement							
GBM	1.6[b]	72.4	0.1[b]	1.4	4.5[b]	47.4	40.6
PCNSL	60.9	93.0[a]	8.8[a]	0.4	63.7	92.2[a]	87.7[a]
Metastasis	13.2	82.4	0.8	1.1	31.8	60.4	55.8
Cystic appearance							
GBM	30.7	77.6	1.4	0.9	52.8	57.9	56.5
PCNSL	0.0[b]	68.7	0.0[b]	1.5	0.0[b]	77.4[b]	57.2
Metastasis	32.1	77.7	1.4	0.9	47.2	64.7	60.2
Central necrosis							
GBM	79.0[a]	65.8	2.3	0.3[a]	65.3[a]	79.4	71.4[a]
PCNSL	39.1	42.6	0.7	1.4	12.0	77.7	42.0
Metastasis	32.0	31.8	0.5	2.1	22.7	42.9	31.9
Intratumoral hemorrhage							
GBM	33.9	82.9[a]	2.0	0.8	61.7[a]	60.6	60.9
PCNSL	4.4[b]	71.3	0.2	1.3	3.0[b]	78.8[b]	60.1
Metastasis	22.6	74.1	0.9	1.0	35.3	60.6	54.4
Abnormal flow void							
GBM	58.1	84.2[a]	3.7	0.5	75.0[a]	71.1	72.5
PCNSL	8.7	60.0	0.2	1.5	4.2	76.6	51.4
Metastasis	18.9	55.3	0.4	1.5	20.8	52.2	41.3
Presence of hypointensity component on precontrast T1W MRI							
GBM	90.6[a]	36	1.4	0.3	53.6	82.5[a]	60.5
PCNSL	72.7	19.6	0.9	1.4	15.4	78.2	28.4
Metastasis	72.7	19.6	0.9	1.4	36.1	53.5	40.0

(*Continued*)

Table 3 (*Continued*)

Variables	Sensitivity (%)	Specificity (%)	LR+	LR−	PPV (%)	NPV (%)	Accuracy (%)
Presence of isointensity component on FLAIR MRI							
GBM	12.5	72	0.5	1.2	26.7	50.2	45.3
PCNSL	9.1	78.3	0.4	1.2	7.7	81.1	66.7
Metastasis	54.6	89.1[a]	5.0[a]	0.5	75.8[a]	75.9	75.9
Presence of hypodensity component on NCECT							
GBM	85.3[a]	19.2	1.0	0.8	46.2	61.5	48.9
PCNSL	60.0	14.1	0.7	2.8	12.3	63.7	21.8
Metastasis	86.5[a]	20.5	1.1	0.7	40.4	70.8	45.8
Presence of isodensity component on NCECT							
GBM	35.3	25.5	0.5	2.5	27.9	32.6	29.9
PCNSL	91.7[a]	47.8	1.8	0.2[a]	26.1	96.6[a]	55.2
Metastasis	64.9	47.7	1.2	0.7	43.6	68.5	54.3

Abbreviations: FLAIR, fluid-attenuated inversion recovery; GBM, glioblastoma; LR −, negative likelihood ratio; LR +, positive likelihood ratio; MRI, magnetic resonance imaging; NCECT, noncontrast-enhanced computerized tomography; NPV, negative predictive value; PCNSL, primary central nervous system lymphoma; PPV, positive predictive value; T1W, T1-weighted.
[a]Value with dominant positive relationship between the individual variable and tumor.
[b]Value with dominant negative relationship between the individual variable and tumor.

PCNSL and unlikely to be GBM. Similarly, in the variable of infratentorial tumor location, high specificity, LR +, PPV, and accuracy were found in metastatic tumor but GBM exhibiting low sensitivity, LR +, PPV, and accuracy. We could interpret that a solitary contrast-enhancing tumor located in the posterior cranial fossa carried an outstanding possibility of being metastasis and a weak possibility of being GBM.

Discussion

The most common primary malignant brain tumor is GBM.[7,8] Brain metastasis is a tumor that is being increasingly found in cancer survivors, whereas PCNSL is a relatively rare entity with an aggressive course.[9] Patients with any of these three types of tumors can present with a solitary contrast enhancing intracranial tumor. With some patients who have brain imaging showing this finding, difficulty in differentiating between the three tumor types are encountered. There are no pathognomonic findings to distinguish between each of the individual types of tumors. The authors conducted this study to establish the predictive factors for GBM, PCNSL, and metastasis. Our results may be useful for the preoperative decision-making related to the neurosurgical management of these intracranial malignant lesions. In patients with GBM and single brain metastasis arising in an accessible location, total surgical removal remains the treatment of choice. In cases harboring lesions with the high possibility of being intracranial lymphoma, tissue biopsy without resection is appropriate for treatment with chemotherapy or radiation therapy. Surgical resection of PCNSL is not helpful in improving survival outcomes.[10]

In our study, several predictors were found to be associated with the possibility of being GBM. The tumor size was significantly larger in GBM because this type of tumor usually grows rapidly and is found when it is large, resulting in rapidly progressing symptoms of increasing intracranial pressure or neurological deficits. The tumor margin of GBM was also irregular compared with PCNSL and metastasis (►**Fig. 1A**). GBM is an infiltrative high-grade glioma, and tumor cells can be found in the peritumoral area. These properties of GBM may make the tumor margin more irregular than those of the other types of tumor. After contrast injection, almost all instances of GBM in our study (98.4%) showed heterogeneous contrast enhancement (►**Fig. 1B**). Contrast-enhanced component represents the highly vascularized portion of GBM, whereas the area without contrast enhancement represents central necrosis (►**Fig. 1C**), which was significantly associated with GBM in the present study. As to intratumoral hemorrhage, Ding et al found that the intratumoral hemorrhagic burden and the number of vessels within the tumors detected by susceptibility-weighted imaging were significantly higher in high-grade gliomas and metastasis than those in PCNSL. They also demonstrated that there was no significant difference in these two variables of high-grade glioma and metastasis.[11] Our study had similar results. Intratumoral hemorrhage (►**Fig. 1D**) and abnormal tumor flow void (►**Fig. 1E**) were significantly prominent in the GBM group. As to the aforementioned highly vascularized properties of GBM, the prominent vascular structures are represented as tumor flow void and may result in intratumoral hemorrhagic phenomenon. Nevertheless, characteristics of tumor flow void were not significantly different between the tumor groups. Furthermore, hypodensity component on noncontrast-enhanced cranial CT associated with GBM may indicate some parts of central necrosis and cystic component within the tumor (►**Fig. 1F**).

Turning to the analysis of the peritumoral area, Maurer et al showed that the ratio of the maximum diameter of the

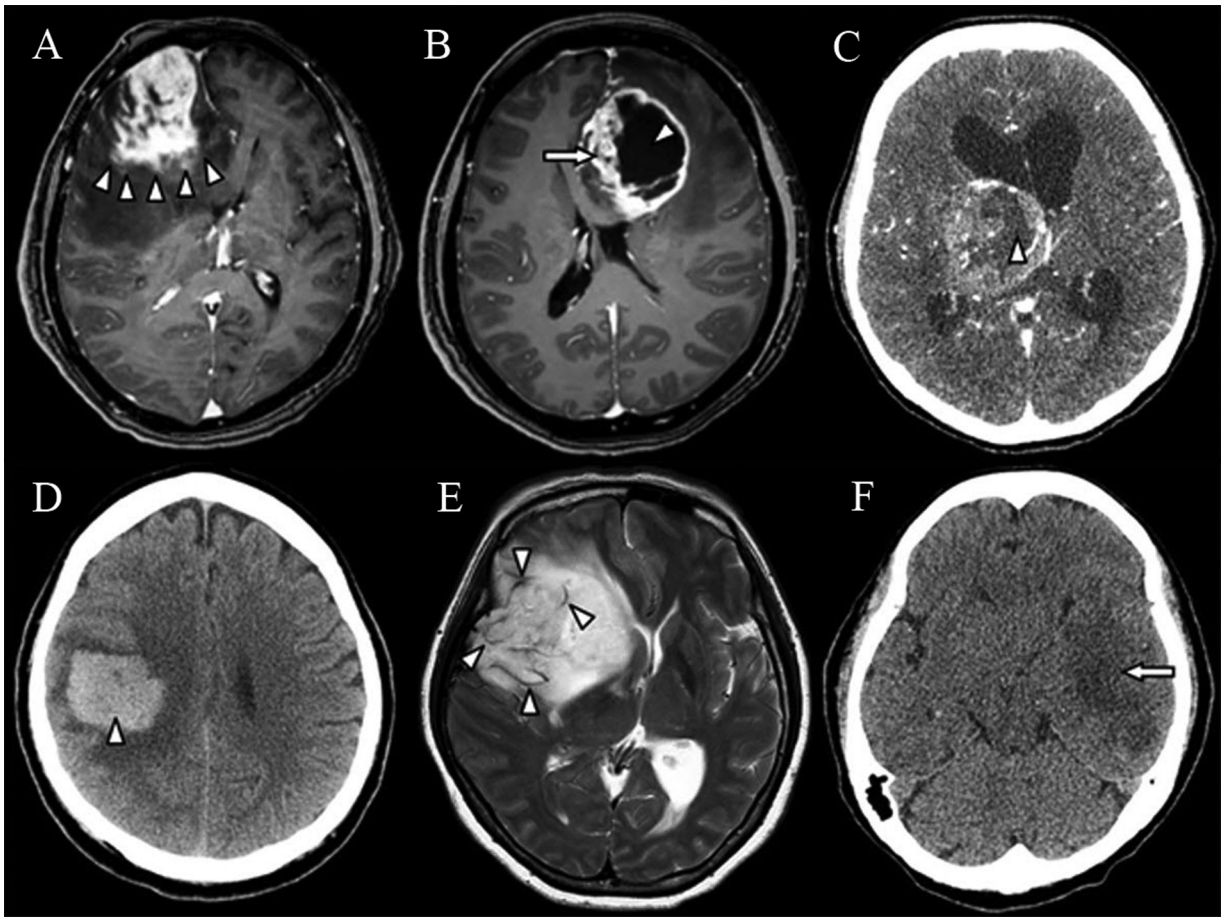

Fig. 1 Cranial images of patients with GBM. (**A**) GBM with irregular margin (arrowheads) on contrast-enhanced T1W MRI; (**B**) contrast-enhanced T1W MRI showing heterogeneous enhancement, including solid (arrow) and cystic (arrowhead) components; (**C**) central necrosis (arrowhead) on contrast-enhanced CT; (**D**) intratumoral hemorrhage (arrowhead) on noncontrast-enhanced CT; (**E**) abnormal flow void (arrowhead) on T2W MRI; (**F**) hypodensity component (arrow) on noncontrast-enhanced CT. CT, computed tomography; GBM, glioblastoma; MRI, magnetic resonance imaging; T1W, T1-weighted; T2W, T2-weighted.

peritumoral area on T2W MRI (d T2) to the maximum diameter of the enhancing mass area on postcontrast T1W MRI (d T1 postcontrast) was useful in differentiating between GBM and metastasis. A lower d T2/d T1 postcontrast ratio with a cutoff point of 2.35 favored the possibility of the tumor being GBM.[12] However, the usefulness of the degree of peritumoral brain edema, measured by our method, in differentiating between the three tumor types could not be confirmed by our study.

PCNSL, a relatively rare intracranial malignant neoplasm, is found in 5% of all primary brain tumors.[13] It may masquerade as other diseases, or it may have atypical imaging characteristics.[14] In our study, the most common location of PCNSL was the supratentorial region. A deep-seated location—particularly the periventricular areas, basal ganglia, or corpus callosum (►**Fig. 2A–D**)—was more common with PCNSL than GBM or metastasis. The involvement of the cerebellum and brainstem was uncommon in our PCNSL group. Our results corresponded with those of other studies.[15–17] Because of the high nuclear-to-cytoplasmic ratio, PCNSL typically showed hyperdensity or isodensity in the CT scans (►**Fig. 2E**), hypointensity on precontrast T1W MRI, and homogeneous enhancement following contrast injection (►**Fig. 2F**).[16] Necrotic areas and intratumoral hemorrhage are rare in PCNSL.[14] We also found these findings in our PCNSL group.

A few predictors of metastasis were found by our study. Of them, the predictors with a high strength of association included an infratentorial tumor location (►**Fig. 3A**) and a smooth tumor margin (►**Fig. 3B, C**). GBM and PCNSL are uncommon tumors arising in the posterior cranial fossa. Therefore, if a solitary enhancing tumor is found at the cerebellum, it has a greater possibility of being a metastatic lesion than GBM or PCNSL. Additionally, most metastatic tumors have well-defined borders, so circumferential complete tumor resection without resection of the surrounding brain can be performed in such cases.

Many studies have demonstrated that the rCBV in GBM and metastasis was greater than the rCBV in PCNSL.[18–20] Nevertheless, our study did not find a significant difference in the rCBVs of the three tumor groups. Almost all patients in the three groups had a high rCBV. This may be a result of having too small analyzed cases of rCBV, particularly in the PCNSL and metastatic groups; this is acknowledged as being a limitation of our study.

The role of advanced imaging studies has been steadily increasing. Various MRI sequences are helpful in

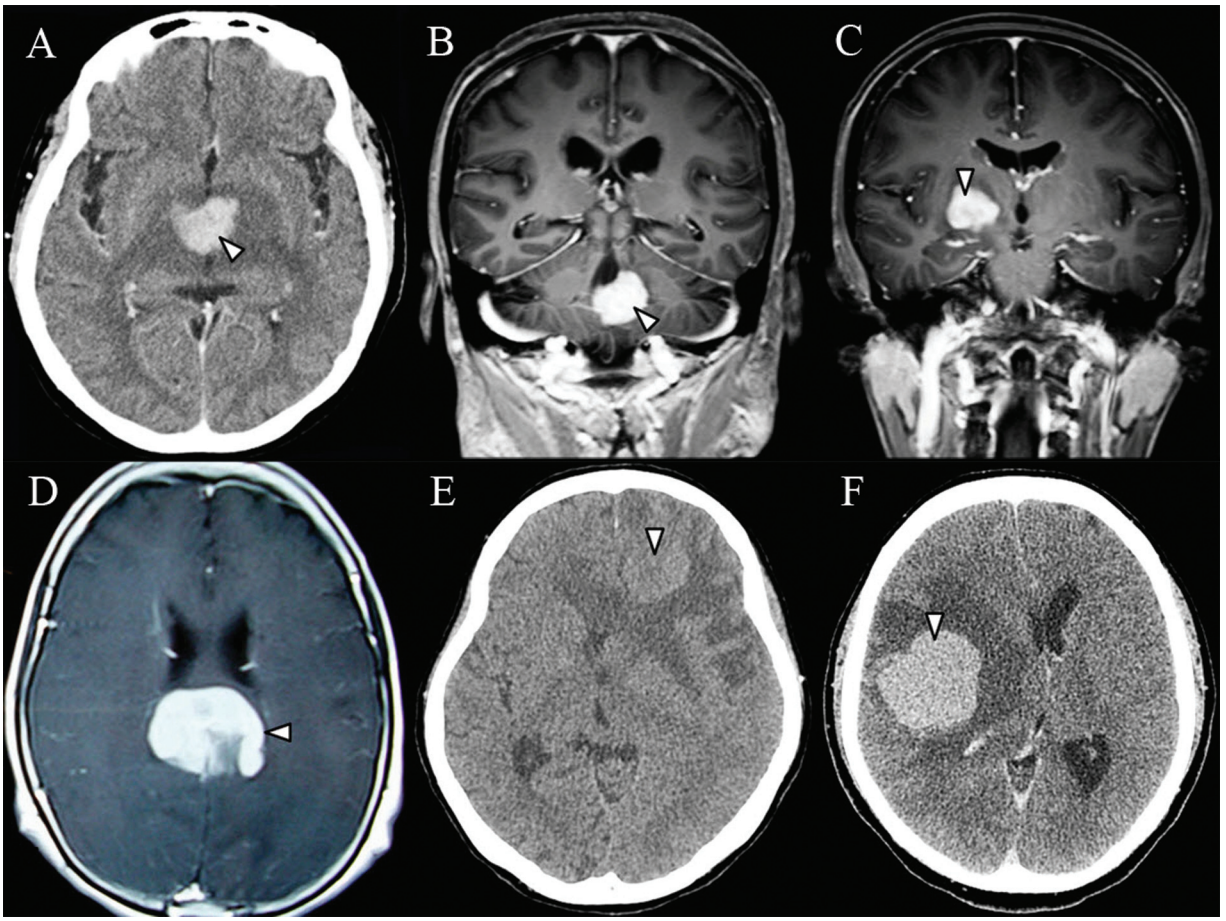

Fig. 2 Cranial images of patients with PCNSL. (**A**) Contrast-enhanced CT and (**B**) contrast-enhanced T1W MRI showing the periventricular location of a tumor (arrowhead); (**C**) contrast-enhanced T1W MRI showing basal ganglial involvement (arrowhead); (**D**) lymphoma involving the splenium of the corpus callosum (arrowhead) on T1W MRI after contrast injection; (**E**) tumor with isodensity appearance (arrowhead) on noncontrast-enhanced CT; (**F**) contrast-enhanced CT showing homogeneous enhancement of a tumor (arrowhead). CT computed tomography; MRI, magnetic resonance imaging; PCNSL, primary central nervous system lymphoma; T1W, T1-weighted.

differentiating between GBM, PCNSL, and metastasis, for instance, apparent diffusion coefficient,[21,22] dynamic contrast-enhanced MRI,[23–25] perfusion MRI,[26,27] diffusion tensor imaging,[23,28] diffusion-weighted imaging,[29] a whole-tumor histogram analysis of normalized cerebral blood volume,[3,22] and arterial spin labeling.[25,29] Additionally, fluorodeoxyglucose positron emission tomography (^{18}F-FDG PET)/CT is a helpful radiographic tool for the detection of an extracranial involvement of lymphoma and the differentiation of lymphoma from GBM and metastasis. Lymphoma

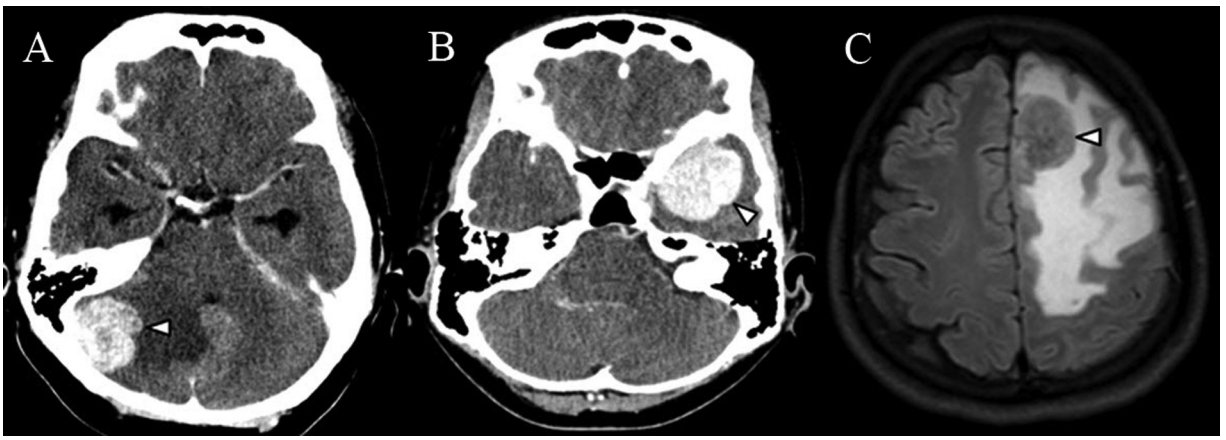

Fig. 3 Cranial images of patients with brain metastasis. (**A**) Contrast-enhanced CT revealing a tumor arising in the posterior cranial fossa (arrowhead); (**B**) contrast-enhanced CT, and (**C**) FLAIR MRI showing smooth margin of a tumor (arrowhead). CT, computed tomography; FLAIR, fluid-attenuated inversion recovery; MRI, magnetic resonance imaging.

Table 4 Variables supporting or opposing possibility of being glioblastoma, primary central nervous system lymphoma, and metastasis

Variables	GBM	PCNSL	Metastasis
Seizure	+	−	
Functional impairment		+	
Infratentorial tumor location	−−		++
Deep-seated tumor location		++	−
Smooth tumor margin		+	++
Homogeneous contrast enhancement	−−	++	
Cystic appearance		−−	
Central necrosis	+		
Intratumoral hemorrhage	+	−	
Abnormal flow void	+		
Presence of hypointensity component on precontrast T1W MRI	+		
Presence of isointensity component on FLAIR MRI			+
Presence of hypodensity component on NCECT	+		+
Presence of isodensity component on NCECT		+	

Abbreviations: FLAIR, fluid-attenuated inversion recovery; GBM, glioblastoma; MRI, magnetic resonance imaging; NCECT, noncontrast-enhanced computerized tomography; PCNSL, primary central nervous system lymphoma; T1W, T1-weighted.
+Variable supporting possibility of being the tumor.
++Variable greatly supporting possibility of being the tumor.
−Variable opposing possibility of being the tumor.
−−Variable greatly opposing possibility of being the tumor.

has shown a significantly high metabolic uptake compared with GBM and metastasis.[2,29,30] Recently, machine learning models have been used for differentiating GBM, PCNSL, and metastasis. Several studies showed useful of the models in preoperative prediction of the tumor types.[31–33] In current clinical practice, it would be practical to interpret the difference between these tumors using these advanced imaging techniques. Even though these advanced tools are useful in differentiating between these tumors with overlapping features, they are not generally available and require skilled interpreters. By comparison, our predictors are easily feasible because they are based on common clinical characteristics and radiographic features on imaging studies. Regarding the analyzed data obtained from ►**Tables 1**, **2**, and **3**, variables either supporting or opposing possibility of being GBM, PCNSL, and metastasis are summarized in ►**Table 4**. These variables are helpful and can be used as strong predictors for distinguishing between the three types of malignant brain tumor. Furthermore, the literature review regarding predictors of being GBM, PCNSL, and metastasis are summarized in ►**Table 5**.

A major limitation of the study should be mentioned. Some neuroimaging modalities, including cranial MRI, cranial CT, and measurement of the rCBV, were available in not all cases. Therefore, analyzed population numbers were different between these modalities. The heterogeneity in population numbers may affect results of data analysis of some variables. In the future, research in homogeneous study group should be conducted.

Conclusion

Our study established useful predictors to differentiate between GBM, PCNSL, and metastasis. The predictors of being GBM are functional impairment, large tumor size, irregular tumor margin, heterogeneous contrast enhancement, central necrosis, intratumoral hemorrhage, abnormal flow void, presence of hypointensity component on precontrast cranial T1W MRI, and hypodensity component on noncontrast cranial CT. The predictors of being PCNSL comprise functional impairment, deep-seated tumor location, homogeneous contrast enhancement, absence of cystic appearance, and presence of isodensity component on noncontrast cranial CT. Finally, the predictors of being metastasis are an infratentorial or extra-axial tumor location, smooth tumor margin, and presence of isointensity component on cranial FLAIR MRI.

Authors' Contributions

P.C.: development or design of methodology, project administration, software, investigation, data collection, formal analysis, visualization, writing—original draft preparation, and approval of the final manuscript; B.S.: conceptualization, development or design of methodology, supervision, formal analysis, writing—reviewing and editing, corresponding author, and approval of the final manuscript; T.W.: writing—reviewing and editing, and approval of the final manuscript; C.T.: writing—reviewing and editing, and approval of the final manuscript; I.K.: writing—reviewing and editing, and approval of the final

Table 5 The literature review regarding predictors of being glioblastoma, primary central nervous system lymphoma, and metastasis

Authors, year	Population, *n*	Used method	Compared parameter	Predictor		
				GBM/HGG	PCNSL/lymphoma	Metastasis
Calli et al[18] 2002	Total 48 cases (GBM 17, AA 4, 8 PCNSL, 9 metastasis)	C-MRI, DWI, PWI	ADC_{min}, $rCBV_{max}$	[a]Higher ADC_{min} [a]Higher $rCBV_{max}$	[a]Lower ADC_{min} [a]Lower $rCBV_{max}$	Not different from GBM for ADC_{min} and $rCBV_{max}$
Wang et al[23] 2011	Total 67 cases (GBM 26, PCNSL 16, metastasis 25)	DTI, DSC-MRI	ADC, FA, CL, CP, CS, rCBV, $rCBV_{max}$	[a]Higher ADC in ER [a]Higher FA in ER, IPR, DPR [a]Higher CL in ER, IPR [a]Higher CP in ER, IPR, DPR [a]Lower CS in ER, IPR [a]Higher rCBV in ER, IPR [a]Higher $rCBV_{max}$ in ER, IPR	[a]Lower ADC in ER [a]Lower FA in ER, IPR, DPR [a]Lower CL in ER, IPR [a]Lower CP in ER, IPR, DPR [a]Higher CS in ER, IPR [a]Lower rCBV in ER, IPR [a]Lower $rCBV_{max}$ in ER, IPR	[a]High ADC in ER [a]Lower FA in ER, IPR [a]Lower CL in ER, IPR [a]Lower CP in ER, IPR, DPR [a]Higher CS in ER, IPR [a]Lower rCBV in IPR [a]Lower $rCBV_{max}$ in IPR Not difference from GBM for FA in DPR; rCBV in ER, DPR; $rCBV_{max}$ in ER, DPR
Neska-Matuszewska et al[20] 2018	Total 74 cases (GBM 27, PCNSL 17, metastasis 30)	DWI, PWI	ADC, rCBV, rPH, rPSR	[a]Higher ADC_{mean} [a]Higher ADC_{min} [a]Higher $rCBV_{mean}$ [a]Higher $rCBV_{max}$ [a]Higher rPH_{mean} [a]Higher rPH_{max} [a]Lower $rPSR_{mean}$ [a]Lower $rPSR_{max}$	[a]Lower ADC_{mean} [a]Lower ADC_{min} [a]Lower $rCBV_{mean}$ [a]Lower $rCBV_{max}$ [a]Lower rPH_{mean} [a]Lower rPH_{max} [a]Higher $rPSR_{mean}$ [a]Higher $rPSR_{max}$	Not different from GBM for ADC_{mean}, ADC_{min}, $rCBV_{mean}$, $rCBV_{max}$, rPH_{mean}, rPH_{max}, $rPSR_{mean}$, $rPSR_{max}$
Lee et al[34] 2019	Total 54 cases (GBM 14, PCNSL 7, metastasis 20, meningioma 13)	DSC-MRI	rCBV, PSR, normalized baseline signal intensity	rCBV was better than PSR in differentiating GBM from PCNSL, and meningioma from GBM rCBV and PSR were poor in differentiating GBM from metastasis Normalized baseline signal intensity was better than rCBV and PSR differentiating GBM from metastasis	PSR was better than rCBV in differentiating PCNSL from metastasis rCBV and PSR were similar in differentiating PCNSL from GBM or meningioma	rCBV was better than PSR in differentiating metastasis from meningioma

Table 5 (*Continued*)

Authors, year	Population, *n*	Used method	Compared parameter	Predictor		
				GBM/HGG	PCNSL/lymphoma	Metastasis
Eyüboğlu et al[35] 2021	Total 125 cases (HGG 55, LGG 22, lymphoma 16, metastasis 32)	DWI	ADC_t, ADC_t ratio, ADC_{tch}, ADC_{tch} ratio	HGG showing [a]Lower ADC_{tch} [a]Lower ADC_{tch} ratio Not different from lymphoma and metastasis for ADC_t and ADC_t ratio	[a]Higher ADC_{tch} [a]Higher ADC_{tch} ratio	[a]Higher ADC_{tch} [a]Higher ADC_{tch} ratio
Bilgin and Ünal[36] 2023	Total 39 cases (GBM 13, PCNSL 13, metastasis 13)	C-MRI, DWI	Edema–mass ratio, ADC in lesion and perilesional area	[a]Lower edema–mass ratio [a]Higher ADC in lesion Not different from PCNSL and metastasis for ADC in perilesional area	[a]Higher edema–mass ratio [a]Lower ADC in lesion	[a]Higher edema–mass ratio Not different from GBM for ADC in lesion
Ma et al[3] 2010	Total 59 cases (GBM 28, lymphoma 12, metastasis 22)	C-MRI, DSC-MRI	HW, PHP, and MV of CBV	For contrast-enhancing lesion [a]Higher HW [a]Higher PHP [a]Higher MV For perienhancing lesion [a]Higher HW [a]Higher PHP [a]Higher MV	For contrast-enhancing lesion [a]Lower HW [a]Lower PHP [a]Lower MV For perienhancing lesion [a]Lower HW [a]Lower PHP [a]Lower MV	For contrast-enhancing lesion, not different from GBM for higher HW, PHP, and MV For perienhancing lesion [a]Lower HW [a]Lower PHP [a]Lower MV
Goyal et al[37] 2017	Total 56 cases (GBM 18, lymphoma 15, metastasis 13, AEG 10)	DSC-MRPI	CBV_{mean}, CBV_{max}	[a]Higher CBV_{mean} [a]Higher CBV_{max}	[a]Lower CBV_{mean} [a]Lower CBV_{max}	[a]Higher CBV_{mean} [a]Higher CBV_{max} Not compared with GBM for CBV_{mean}, CBV_{max}
Xi et al[25] 2019	Total 35 cases (HGG 21, PCNSL 8, metastasis 6)	C-MRI, ASL, DCE-MRI	CBF, rCBF, K^{trans}, V_e	HGG showing [a]Higher CBF [a]Higher rCBF [a]Lower K^{trans} [a]Lower V_e	[a]Lower CBF [a]Lower rCBF [a]Higher K^{trans} [a]Higher V_e	[a]Higher CBF [a]Higher rCBF [a]Lower K^{trans} [a]Lower V_e
Onishi et al[19] 2018		Perfusion CT				

(*Continued*)

Table 5 (*Continued*)

Authors, year	Population, *n*	Used method	Compared parameter	Predictor		
				GBM/HGG	PCNSL/lymphoma	Metastasis
	Total 39 cases (GBM 22, PCNSL 6, metastasis 11)		rCBFt, rCBVt, rCBFp, rCBVp, rMTTt	[a]Higher rCBFt [a]Higher rCBVt [a]Higher rCBFp [a]Higher rCBVp [a]Lower rMTTt	[a]Lower rCBFt [a]Lower rCBVt Higher rCBFp Higher rCBVp [a]Lower rMTTt	[a]Lower rCBFt [a]Lower rCBVt [a]Lower rCBFp [a]Lower rCBVp [a]Higher rMTTt
Ding et al[11] 2014	Total 104 lesions (HGG 35, PCNSL 23, metastasis 46)	C-MRI, SWI	Intralesional hemorrhagic burden, number of intralesional vessel	[a]Higher intralesional hemorrhagic burden and number of intralesional vessel for HGG	[a]Lower intralesional hemorrhagic burden and number of intralesional vessel	Not different from HGG for intralesional hemorrhagic burden and number of intralesional vessel
Lu et al[24] 2016	Total 75 cases (GBM 38, PCNSL 16, metastasis 21)	DCE-MRI	K^{trans}, V_e	[a]Lower K^{trans} [a]Lower V_e	[a]Higher K^{trans} [a]Higher V_e	[a]Lower K^{trans} [a]Lower V_e
Das et al[38] 2011	Total 20 cases (GBM 8, LGG 7, PCNSL 1, metastasis 4)	^{18}F-FDG PET/CT	SUV_{avg}, SUV_{max}	[a]Lower SUV_{avg} [a]Lower SUV_{max}	[a]Higher SUV_{avg} [a]Higher SUV_{max} SUV_{max} of 15.0 was cutoff for diagnosis of PCNSL	Metastasis showing higher SUV_{avg} and SUV_{max} than GBM
Meric et al[39] 2015	Total 76 cases (HGG 18, PCNSL 6, metastasis 52)	^{18}F-FDG PET/CT	SUV_{avg}, SUV_{max}, T_{max}:Ci_{max}, T_{max}:Cc_{max}, T_{max}:WMi_{max}, T_{max}:WMc_{max}, T_{avg}:Ci_{avg}, T_{avg}:Cc_{avg}, T_{avg}:WMi_{avg}, T_{avg}:WMc_{avg}	[a]Lower for all parameters than PCNSL [a]Lower for T_{max}:Ci_{max}, T_{max}:Cc_{max}, T_{max}:WMi_{max}, T_{avg}:Ci_{avg}, T_{avg}:Cc_{avg}, T_{avg}:WMi_{avg}, T_{avg}:WMc_{avg} than metastasis	[a]Higher for all parameters than HGG [a]Higher for SUV_{avg}, SUV_{max}, T_{max}:Ci_{max}, T_{max}:Cc_{max}, T_{max}:WMi_{max}, T_{avg}:Ci_{avg} than metastasis	[a]Higher for T_{max}:Ci_{max}, T_{max}:Cc_{max}, T_{max}:WMi_{max}, T_{avg}:Ci_{avg}, T_{avg}:Cc_{avg}, T_{avg}:WMi_{avg}, T_{avg}:WMc_{avg} than HGG [a]Lower for SUV_{avg}, SUV_{max}, T_{max}:Ci_{max}, T_{max}:Cc_{max}, T_{max}:WMi_{max}, T_{avg}:Ci_{avg} than PCNSL
Purandare et al[2] 2017	Total 101 cases (GBM 30, lymphoma 25, metastasis 46)	^{18}F-FDG PET/CT	SUV_{max}, tumor to background activity ratio	[a]Lower SUV_{max} [a]Lower tumor to background activity ratio	[a]Higher SUV_{max} [a]Higher tumor to background activity ratio	[a]Lower SUV_{max} [a]Lower tumor to background activity ratio

Table 5 (*Continued*)

Authors, year	Population, *n*	Used method	Compared parameter	Predictor		
				GBM/HGG	PCNSL/lymphoma	Metastasis
Wang et al[40] 2022	Total 192 cases (GBM 70, PCNSL 41, metastasis 81)	Age, blood test	Age, platelet count in CBC, LDH, β2-MG, α2-G, INR, TT, FDP	[a]Lower INR and higher TT than for PCNSL and metastasis Accuracy of diagnostic model was 76.1%	Accuracy of diagnostic model was 22%	[a]Older age and lower platelet count than for GBM Accuracy of diagnostic model was 88.2%
The present study	Total 138 (GBM 62, PCNSL 23, metastasis 53)	Clinical variables, NCECT, CECT, C-MRI	Clinical variables, tumor location, and characteristics on neuroimaging	[a]Presence of seizure [a]Central necrosis [a]Intratumoral hemorrhage [a]Abnormal flow void [a]Presence of hypointensity component on precontrast T1W MRI	[a]Functional impairment [a]Deep-seated tumor location [a]Smooth tumor margin [a]Homogeneous contrast enhancement [a]Presence of isodensity component on NCECT	[a]Infratentorial tumor location [a]Smooth tumor margin [a]Presence of isointensity component on FLAIR [a]Presence of hypodensity component on NCECT

Abbreviations: AA, anaplastic astrocytoma; ADC, apparent diffusion coefficient; ADC_{mean}, mean apparent diffusion coefficient; ADC_{min}, minimum apparent diffusion coefficient; ADC_t, apparent diffusion coefficient from tumor; ADC_{tch}, apparent diffusion coefficient from tumor circumferential hyperintensity; AEG, anaplastic enhancing glioma; ASL, arterial spin labeling; CBC, complete blood count; CBV, cerebral blood volume; CBV_{max}, maximum cerebral blood volume; CBV_{mean}, mean cerebral blood volume; CECT, contrast-enhanced computerized tomography; CEMRI, contrast-enhanced magnetic resonance imaging; CL, linear anisotropy coefficient; C-MRI, conventional magnetic resonance imaging; CP, planar anisotropy coefficient; CS, spheric anisotropy coefficient; CT, computed tomography; DCE-MRI, dynamic contrast-enhanced magnetic resonance imaging; DPR, distant peritumoral region; DSC-MRI, dynamic susceptibility contrast-enhanced magnetic resonance imaging; DSC-MRPI, dynamic susceptibility-weighted magnetic resonance perfusion imaging; DTI, diffusion tensor imaging; DWI, diffusion-weighted imaging; ER, enhancing region; FA, fractional anisotropy; FDG PET, fluorodeoxyglucose positron emission tomography; FDP, fibrin degradation product; FLAIR, fluid-attenuated inversion recovery; GBM, glioblastoma; HGG, high grade glioma; HW, histogram width; INR, international normalized ratio; IPR, immediate peritumoral region; K^{trans}, volume transfer constant; LDH, lactate dehydrogenase; LGG, low-grade glioma; MV, maximum value; NCECT, noncontrast-enhanced computerized tomography; PCNSL, primary central nervous system lymphoma; PHP, peak height position; PSR, percentage signal recovery; PWI, perfusion-weighted imaging; rCBFp, relative cerebral blood flow in peritumoral region; rCBFt, relative cerebral blood flow in tumor; rCBV, relative cerebral blood volume; $rCBV_{max}$, maximum relative cerebral blood volume; $rCBV_{mean}$, mean relative cerebral blood volume; rCBVp, relative cerebral blood volume in peritumoral region; rCBVt, relative cerebral blood volume in tumor; rMTTt, relative mean transit time in tumor; rPH, relative peak height; rPH_{max}, maximum relative peak height; rPH_{mean}, mean relative peak height; rPSR, relative percentage of signal recovery; $rPSR_{max}$, maximum relative percentage of signal recovery; $rPSR_{mean}$, mean relative percentage of signal recovery; SUV_{avg}, average standardized uptake value; SUV_{max}, maximum standardized uptake value; SWI, susceptibility-weighted imaging; T1W, T1-weighted; T_{avg}:Cc_{avg}, the tumor SUV_{avg} to contralateral cortex SUV_{avg} ratio; T_{avg}:Ci_{avg}, the tumor SUV_{avg} to ipsilateral cortex SUV_{avg} ratio; T_{avg}:WMc_{avg}, the tumor SUV_{avg} to contralateral white matter SUV_{avg} ratio; T_{avg}:WMi_{avg}, the tumor SUV_{avg} to ipsilateral white matter SUV_{avg} ratio; T_{max}:Cc_{max}, the tumor SUV_{max} to contralateral cortex SUV_{max} ratio; T_{max}:Ci_{max}, the tumor SUV_{max} to ipsilateral cortex SUV_{max} ratio; T_{max}:WMc_{max}, the tumor SUV_{max} to contralateral white matter SUV_{max} ratio; T_{max}:WMi_{max}, the tumor SUV_{max} to ipsilateral white matter SUV_{max} ratio; TT, thrombin time; V_e, extravascular extracellular volume; α2-G, α2-globulin; β2-MG, β2-macroglobulin.

[a]Statistically significant difference when compared with other type(s) of tumor in the same study.

manuscript; S.N.: writing—reviewing and editing, and approval of the final manuscript.

Ethical Approval

This study was approved by the Ethics Committee of the Faculty of Medicine Siriraj Hospital, Mahidol University, Thailand; Certificate of Approval (COA) number SI 556/2014. All the patients' data retained full confidentiality in compliance with the Declaration of Helsinki.

Funding

None.

Conflict of Interest

None declared.

Acknowledgment

The authors thank Orawan Supapueng, of the Clinical Epidemiology Unit, Office for Research and Development, Faculty of Medicine, Siriraj Hospital, Mahidol University, Bangkok, Thailand for her statistical support.

References

1 Mabray MC, Barajas RF Jr, Cha S. Modern brain tumor imaging. Brain Tumor Res Treat 2015;3(01):8–23
2 Purandare NC, Puranik A, Shah S, et al. Common malignant brain tumors: can 18F-FDG PET/CT aid in differentiation? Nucl Med Commun 2017;38(12):1109–1116
3 Ma JH, Kim HS, Rim NJ, Kim SH, Cho KG. Differentiation among glioblastoma multiforme, solitary metastatic tumor, and lymphoma using whole-tumor histogram analysis of the normalized cerebral blood volume in enhancing and perienhancing lesions. AJNR Am J Neuroradiol 2010;31(09):1699–1706
4 Ling SM, Roach M III, Larson DA, Wara WM. Radiotherapy of primary central nervous system lymphoma in patients with and without human immunodeficiency virus. Ten years of treatment experience at the University of California San Francisco. Cancer 1994;73(10):2570–2582
5 Reni M, Ferreri AJ, Garancini MP, Villa E. Therapeutic management of primary central nervous system lymphoma in immunocompetent patients: results of a critical review of the literature. Ann Oncol 1997;8(03):227–234
6 Herrlinger U, Schabet M, Clemens M, et al. Clinical presentation and therapeutic outcome in 26 patients with primary CNS lymphoma. Acta Neurol Scand 1998;97(04):257–264
7 Lapointe S, Perry A, Butowski NA. Primary brain tumours in adults. Lancet 2018;392(10145):432–446
8 Chandana SR, Movva S, Arora M, Singh T. Primary brain tumors in adults. Am Fam Physician 2008;77(10):1423–1430
9 Siegal T, Bairey O. Primary CNS lymphoma in the elderly: the challenge. Acta Haematol 2019;141(03):138–145
10 Sitthinamsuwan B, Rujimethapass S, Chinthammitr Y, Treetipsatit J. Therapeutic and survival outcomes following treatment of primary central nervous system lymphoma: a 12-year case study. J Neurosurg Sci 2014;58(03):183–190
11 Ding Y, Xing Z, Liu B, Lin X, Cao D. Differentiation of primary central nervous system lymphoma from high-grade glioma and brain metastases using susceptibility-weighted imaging. Brain Behav 2014;4(06):841–849
12 Maurer MH, Synowitz M, Badakshi H, et al. Glioblastoma multiforme versus solitary supratentorial brain metastasis: differentiation based on morphology and magnetic resonance signal characteristics. Röfo Fortschr Geb Röntgenstr Neuen Bildgeb Verfahr 2013;185(03):235–240
13 Miller DC, Hochberg FH, Harris NL, Gruber ML, Louis DN, Cohen H. Pathology with clinical correlations of primary central nervous system non-Hodgkin's lymphoma. The Massachusetts General Hospital experience 1958-1989. Cancer 1994;74(04):1383–1397
14 Tang YZ, Booth TC, Bhogal P, Malhotra A, Wilhelm T. Imaging of primary central nervous system lymphoma. Clin Radiol 2011;66 (08):768–777
15 Erdag N, Bhorade RM, Alberico RA, Yousuf N, Patel MR. Primary lymphoma of the central nervous system: typical and atypical CT and MR imaging appearances. AJR Am J Roentgenol 2001;176 (05):1319–1326
16 Küker W, Nägele T, Korfel A, et al. Primary central nervous system lymphomas (PCNSL): MRI features at presentation in 100 patients. J Neurooncol 2005;72(02):169–177
17 Zhang D, Hu LB, Henning TD, et al. MRI findings of primary CNS lymphoma in 26 immunocompetent patients. Korean J Radiol 2010;11(03):269–277
18 Calli C, Kitis O, Yunten N, Yurtseven T, Islekel S, Akalin T. Perfusion and diffusion MR imaging in enhancing malignant cerebral tumors. Eur J Radiol 2006;58(03):394–403
19 Onishi S, Kajiwara Y, Takayasu T, et al. Perfusion computed tomography parameters are useful for differentiating glioblastoma, lymphoma, and metastasis. World Neurosurg 2018;119: e890–e897
20 Neska-Matuszewska M, Bladowska J, Sąsiadek M, Zimny A. Differentiation of glioblastoma multiforme, metastases and primary central nervous system lymphomas using multiparametric perfusion and diffusion MR imaging of a tumor core and a peritumoral zone-searching for a practical approach. PLoS One 2018;13 (01):e0191341
21 Lu S, Wang S, Gao Q, et al. Quantitative evaluation of diffusion and dynamic contrast-enhanced magnetic resonance imaging for differentiation between primary central nervous system lymphoma and glioblastoma. J Comput Assist Tomogr 2017;41(06): 898–903
22 Bao S, Watanabe Y, Takahashi H, et al. Differentiating between glioblastoma and primary CNS lymphoma using combined whole-tumor histogram analysis of the normalized cerebral blood volume and the apparent diffusion coefficient. Magn Reson Med Sci 2019;18(01):53–61
23 Wang S, Kim S, Chawla S, et al. Differentiation between glioblastomas, solitary brain metastases, and primary cerebral lymphomas using diffusion tensor and dynamic susceptibility contrast-enhanced MR imaging. AJNR Am J Neuroradiol 2011;32(03): 507–514
24 Lu S, Gao Q, Yu J, et al. Utility of dynamic contrast-enhanced magnetic resonance imaging for differentiating glioblastoma, primary central nervous system lymphoma and brain metastatic tumor. Eur J Radiol 2016;85(10):1722–1727
25 Xi YB, Kang XW, Wang N, et al. Differentiation of primary central nervous system lymphoma from high-grade glioma and brain metastasis using arterial spin labeling and dynamic contrast-enhanced magnetic resonance imaging. Eur J Radiol 2019; 112:59–64
26 Xu W, Wang Q, Shao A, Xu B, Zhang J. The performance of MR perfusion-weighted imaging for the differentiation of high-grade glioma from primary central nervous system lymphoma: a systematic review and meta-analysis. PLoS One 2017;12(03): e0173430
27 Suh CH, Kim HS, Jung SC, Choi CG, Kim SJ. Perfusion MRI as a diagnostic biomarker for differentiating glioma from brain metastasis: a systematic review and meta-analysis. Eur Radiol 2018; 28(09):3819–3831
28 Toh CH, Castillo M, Wong AM, et al. Primary cerebral lymphoma and glioblastoma multiforme: differences in diffusion

characteristics evaluated with diffusion tensor imaging. AJNR Am J Neuroradiol 2008;29(03):471–475
29 Yamashita K, Yoshiura T, Hiwatashi A, et al. Differentiating primary CNS lymphoma from glioblastoma multiforme: assessment using arterial spin labeling, diffusion-weighted imaging, and ^{18}F-fluorodeoxyglucose positron emission tomography. Neuroradiology 2013;55(02):135–143
30 Zhou W, Wen J, Hua F, et al. ^{18}F-FDG PET/CT in immunocompetent patients with primary central nervous system lymphoma: differentiation from glioblastoma and correlation with DWI. Eur J Radiol 2018;104:26–32
31 Swinburne NC, Schefflein J, Sakai Y, et al. Machine learning for semi-automated classification of glioblastoma, brain metastasis and central nervous system lymphoma using magnetic resonance advanced imaging. Ann Transl Med 2019;7(11):232
32 Priya S, Liu Y, Ward C, et al. Radiomics-based differentiation between glioblastoma, CNS lymphoma, and brain metastases: comparing performance across MRI sequences and machine learning models. Cancers (Basel) 2021;13:2261
33 Tariciotti L, Caccavella VM, Fiore G, et al. A deep learning model for preoperative differentiation of glioblastoma, brain metastasis and primary central nervous system lymphoma: a pilot study. Front Oncol 2022;12:816638
34 Lee MD, Baird GL, Bell LC, Quarles CC, Boxerman JL. Utility of percentage signal recovery and baseline signal in DSC-MRI optimized for relative CBV measurement for differentiating glioblastoma, lymphoma, metastasis, and meningioma. AJNR Am J Neuroradiol 2019;40(09):1445–1450
35 Eyüboğlu İ, Çakir İM, Aslan S, Sari A. Diagnostic efficacy of apparent diffusion coefficient measurements in differentiation of malignant intra-axial brain tumors. Turk J Med Sci 2021;51(01):256–267
36 Bilgin EY, Ünal O. Differentiation of glioblastoma, brain metastases and central nervous system lymphomas using amount of vasogenic edema and diffusion MR imaging of tumor core and peritumoral zone - searching for a practical approach. J Surg Med 2023;7(07):416–420
37 Goyal P, Kumar Y, Gupta N, et al. Usefulness of enhancement-perfusion mismatch in differentiation of CNS lymphomas from other enhancing malignant tumors of the brain. Quant Imaging Med Surg 2017;7(05):511–519
38 Das K, Mittal BR, Vasistha RK, Singh P, Mathuriya SN. Role of (18)F-fluorodeoxyglucose positron emission tomography scan in differentiating enhancing brain tumors. Indian J Nucl Med 2011;26(04):171–176
39 Meric K, Killeen RP, Abi-Ghanem AS, et al. The use of 18F-FDG PET ratios in the differential diagnosis of common malignant brain tumors. Clin Imaging 2015;39(06):970–974
40 Wang SQ, Yuan Q, Zhang GT, et al. Preoperative blood testing for glioblastoma, brain metastases, and primary central nervous system lymphoma differentiation. Transl Cancer Res 2022;11(01):63–71

